Supporting Information

Design of Fe^{III}-Ln^{III} binuclear complexes using compartmental ligands. Synthesis, crystal structures, magnetic properties and *ab initio* analysis

Alexandru Topor,[a†] Dan Liu,[b†] Catalin Maxim,*[a] Ghenadie Novitchi,[c] Cyrille Train,[c] Zeid A. AlOthman,[d] Abdullah A. S. Al-Kahtani,[d] Liviu Ungur,[e] Le Tuan Anh Ho,*[e] Liviu F. Chibotaru,*[f,d] Marius Andruh*[a,g]

[a] *University of Bucharest, Faculty of Chemistry, Inorganic Chemistry Laboratory, Str. Dumbrava Rosie nr. 23, 020464-Bucharest, Romania*

[b] *Institute of Flexible Electronics, Northwestern Polytechnical University, 127 West Youyi Road, Xi'an, 710072, Shaanxi, China*

[c] *CNRS, Univ. Grenoble Alpes, LNCMI, F-38000 Grenoble, France*

[d] *Chemistry Department, College of Science, King Saud University, P.O. Box 2455, Riyadh 11451, Saudi Arabia*

[e] *Department of Chemistry, National University of Singapore, Block S8 Level 3, 3 Science Drive 3, Singapore 117543*

[f] *Theory of Nanomaterials Group, Department of Chemistry KU Leuven, Celestijnenlaan 200F, 3001 Leuven, Belgium.*

[g] *C. D. Nenitzescu Institute of Organic Chemistry of the Romanian Academy, Splaiul Independentei 202B, Bucharest, Romania*

† These authors contributed equally to this work

Table S1. Continuous Shape Measures for the coordination polyhedron around the Ln^{III} atom

Geometry	**Gd^{III} (1)**	**Tb^{III} (2)**	**Dy^{III} (3)**
HBPY-9	16.706	16.666	16.877
JTC-9	15.366	15.421	15.361
JCCU-9	9.748	9.651	9.614
CCU-9	8.979	8.944	8.966
JCSAPR-9	1.729	1.660	1.571
CSAPR-9	1.128	1.120	1.067
JTCTPR-9	3.235	3.105	3.030
TCTPR-9	2.230	2.157	2.140
JTDIC-9	12.332	12.400	12.519
HH-9	9.639	9.721	9.798
MFF-9	**0.585**	**0.616**	**0.628**

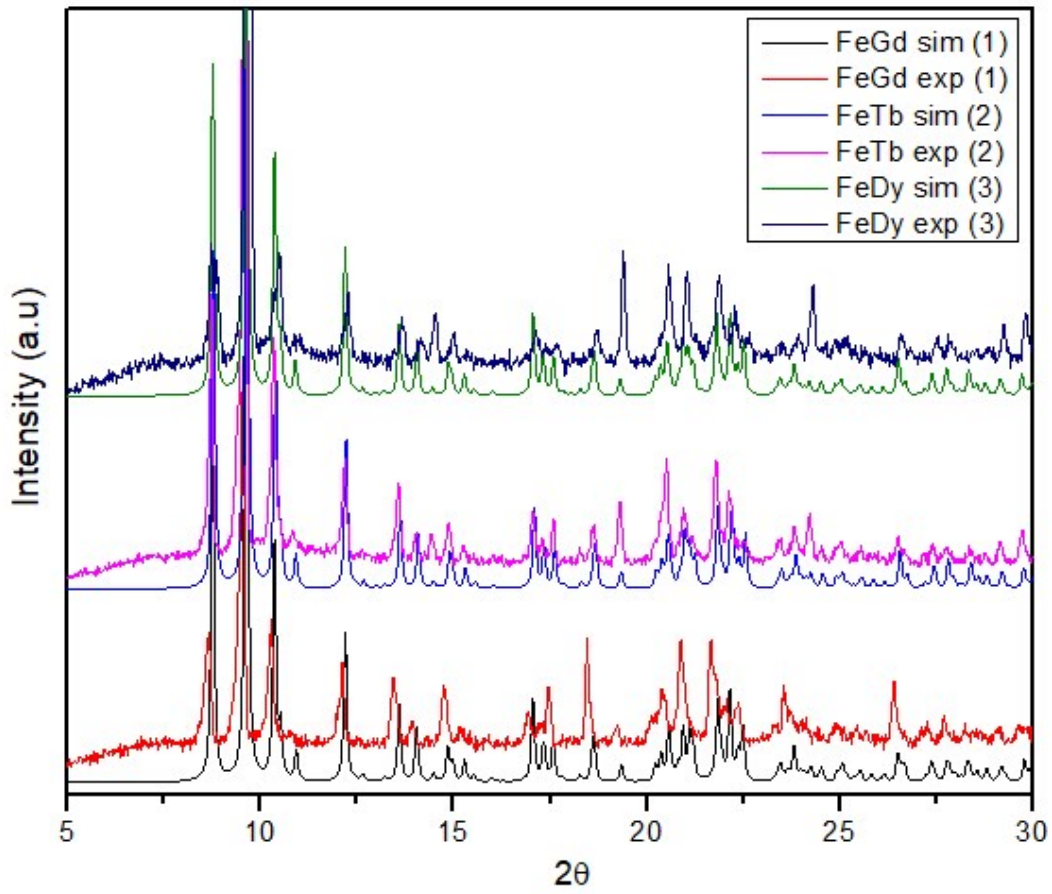

Figure S1. Simulated and experimental powder X-ray diffractograms for compounds **1**, **2** and **3**.

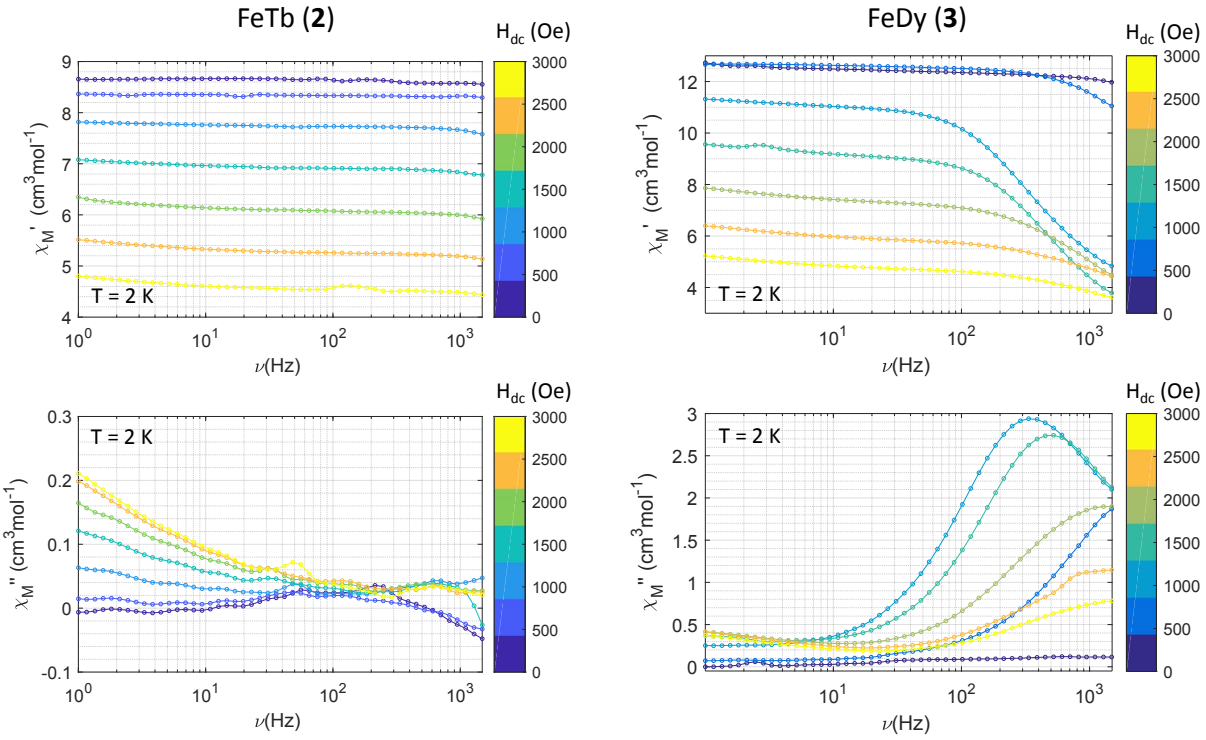

Figure S2. Frequency dependence of the in-phase (upper) and out-of-phase (lower) components of the *ac* magnetic susceptibility for [FeTb] (**2**) (left) and [FeDy] (**3**) (right) at 2 K under different dc fields (0–3000 Oe).

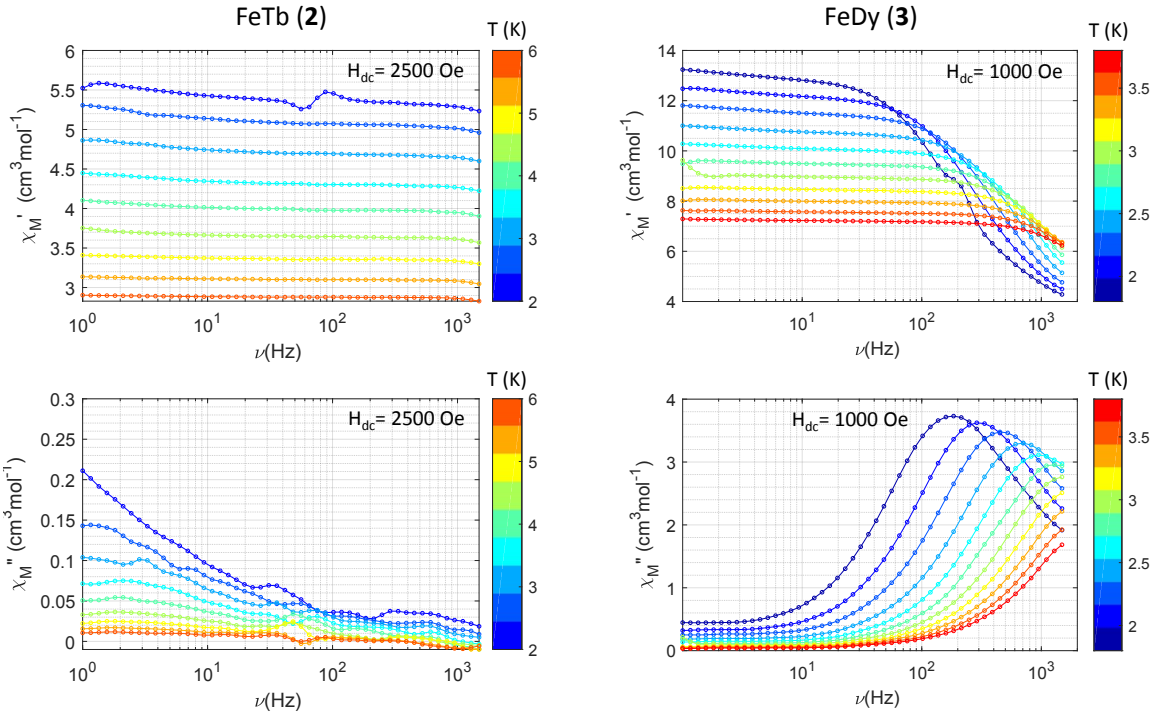

Figure S3. Frequency dependent of the in phase (upper) and out-of-phase (lower) components of the *ac* magnetic susceptibility at different temperatures for [FeTb] (**2**) (left) and [FeDy] (**3**) (right) at respectively 2500 and 1000 Oe *dc* field.

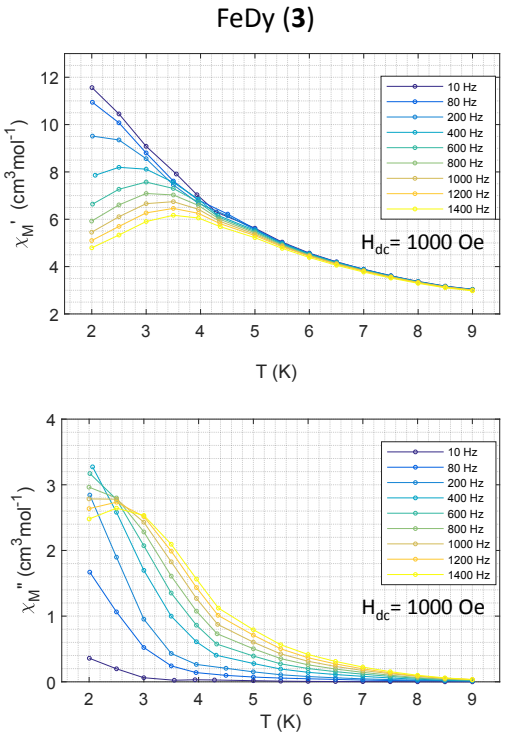

Figure S4. Temperature dependence of the in phase (upper) and out-of-phase (lower) components of the ac magnetic susceptibility at indicated frequency for [FeDy] (**3**) under 1000 Oe *dc* field.

Table S2. Values of the relevant parameters deduced from the best fits of the *ac* susceptibility of [FeDy] (**3**) collected in a 3.0 Oe *ac* field oscillating between 1 and 1500 Hz under 1000Oe *dc* field using the generalized Debye model for a single relaxation process (eq. SI1-2 See Figure 5 in the main text).

	variable parameters				
T(K)	$\chi_{(inf)}$	χ_0	τ(s)	α	R
1.8	3.8167	13.2647	7.304E-04	0.0908	3.459
2.0	3.7235	12.3848	4.706E-04	0.0641	1.7415
2.2	3.5735	11.62	3.222E-04	0.0504	1.1182
2.4	3.4114	10.8133	2.234E-04	0.0384	0.6781
2.6	3.2449	10.1226	1.644E-04	0.0323	0.4523
2.8	2.9345	9.5192	1.240E-04	0.0352	0.3029
3.0	2.916	8.9748	1.013E-04	0.0258	0.2026
3.2	2.5788	8.4751	7.846E-05	0.0308	0.1577
3.4	2.3792	8.0049	6.377E-05	0.0315	0.1103
3.6	2.0915	7.5787	5.149E-05	0.0342	0.0834
3.8	1.7908	7.2341	4.249E-05	0.0386	0.0676

$$\chi'(\nu_{ac}) = \chi_\infty + \frac{(\chi_0 - \chi_\infty)\left[1 + (2\pi\nu_{ac}\tau)^{1-\alpha}\sin(\alpha\pi/2)\right]}{1 + 2(2\pi\nu_{ac}\tau)^{1-\alpha}\sin(\alpha\pi/2) + (2\pi\nu_{ac}\tau)^{2(1-\alpha)}} \quad \text{(eq. SI1)}$$

$$\chi''(\nu_{ac}) = \frac{(\chi_0 - \chi_\infty)(2\pi\nu_{ac}\tau)^{1-\alpha}\cos(\alpha\pi/2)}{1 + 2(2\pi\nu_{ac}\tau)^{1-\alpha}\sin(\alpha\pi/2) + (2\pi\nu_{ac}\tau)^{2(1-\alpha)}} \quad \text{(eq. SI2)}$$

Theoretical calculations.

All calculations were carried out with MOLCAS 8.3 and are of CASSCF/RASSI-SO/SINGLE_ANISO type. The Gd^{III}, Tb^{III}, Dy^{III} and Fe^{III} centers were calculated keeping the entire molecule and using the experimentally determined coordinates of the atoms. Active space of the CASSCF method included 7 electrons in 7 orbitals for Gd^{III}, 8 electrons in 7 orbitals for Tb^{III}, 9 electrons in 7 orbitals for Dy^{III} and 5 electrons in 5 orbitals (4*f* orbitals of Ln^{III} ion and 3d orbital of Fe^{III}). Two basis sets were used in the ab initio calculations, and the detailed information of basis sets were shown in the Table S3-S5 for each fragment of these three complexes.

1. SINGLE-ION MAGNETIC ANISOTROPY

The g-tensors (g-factors and the orientation of the main magnetic axes) as well as the ZFS (orientation of the main anisotropy axes) corresponding to the localized multiplets at the Gd^{III}, Tb^{III}, Dy^{III} and Fe^{III} sites in the [FeTb] [FeTb] and [FeDy] complexes have been calculated with the SINGLE_ANISO module of MOLCAS 8.4 package [1,2]. Tables S6 and S7 show the

energies and the *g*-factors of the four low-lying Kramers doublets of the Gd^{III} ion and Tables S8 and S9 show the same for the three low-lying Kramers doublets of Fe^{III} ion in the [FeGd] complex. Tables S10 and S11 show the energies and the *g*-factors of the low-lying Kramers doublets of the Tb^{III} ion and Tables S12 and S13 show the same for the three low-lying Kramers doublets of Fe^{III} ion in the [FeTb] complex. Tables S14 and S15 show the energies and the *g*-factors of the low-lying Kramers doublets of the Dy^{III} ion and Tables S16 and S17 show the same for the three low-lying Kramers doublets of Fe^{III} ion in the [FeDy] complex.

Table S3. Contractions of the employed basis sets in computational approximations for [FeGd].

Basis 1	Basis 2
GD.ANO-RCC-VDZP	GD.ANO-RCC-VTZP
FE.ANO-RCC-VDZP	FE.ANO-RCC-VTZP
SC.ANO-RCC-VDZP	SC.ANO-RCC-VDZP
LA.ANO-RCC-VDZP	LA.ANO-RCC-VDZP
O.ANO-RCC-VDZP	O.ANO-RCC-VDZP
N.ANO-RCC-VDZP	N.ANO-RCC-VDZP
CL.ANO-RCC-VDZP	CL.ANO-RCC-VDZP
C.ANO-RCC-VDZ	C.ANO-RCC-VDZP
F.ANO-RCC-VDZ	F.ANO-RCC-VDZP
H.ANO-RCC-VDZ	H.ANO-RCC-VDZP

Table S4. Contractions of the employed basis sets in computational approximations for [FeTb].

Basis 1	Basis 2
Tb.ANO-RCC-VDZP	Tb.ANO-RCC-VTZP
FE.ANO-RCC-VDZP	FE.ANO-RCC-VTZP
SC.ANO-RCC-VDZP	SC.ANO-RCC-VDZP
LA.ANO-RCC-VDZP	LA.ANO-RCC-VDZP
O.ANO-RCC-VDZP	O.ANO-RCC-VDZP
N.ANO-RCC-VDZP	N.ANO-RCC-VDZP
CL.ANO-RCC-VDZP	CL.ANO-RCC-VDZP
C.ANO-RCC-VDZ	C.ANO-RCC-VDZP
F.ANO-RCC-VDZ	F.ANO-RCC-VDZP
H.ANO-RCC-VDZ	H.ANO-RCC-VDZP

Table S5. Contractions of the employed basis sets in computational approximations for [FeDy].

Basis 1	Basis 2
Dy.ANO-RCC-VDZP	Dy.ANO-RCC-VTZP
FE.ANO-RCC-VDZP	FE.ANO-RCC-VTZP
LA.ANO-RCC-VDZP	LA.ANO-RCC-VDZP
SC.ANO-RCC-VDZP	SC.ANO-RCC-VDZP
O.ANO-RCC-VDZP	O.ANO-RCC-VDZP
N.ANO-RCC-VDZP	N.ANO-RCC-VDZP
CL.ANO-RCC-VDZP	CL.ANO-RCC-VDZP

C.ANO-RCC-VDZ	C.ANO-RCC-VDZP
F.ANO-RCC-VDZ	F.ANO-RCC-VDZP
H.ANO-RCC-VDZ	H.ANO-RCC-VDZP

[FeGd] complex:

Table S6. Energies of the low-lying doublets (cm^{-1}) of Gd^{III} center in [FeGd] complex.

Spin-orbit energies, cm^{-1}	
Basis 1	Basis 2
0.000	0.000
0.000	0.000
0.198	0.204
0.198	0.204
0.335	0.385
0.335	0.385
0.530	0.671
0.530	0.671

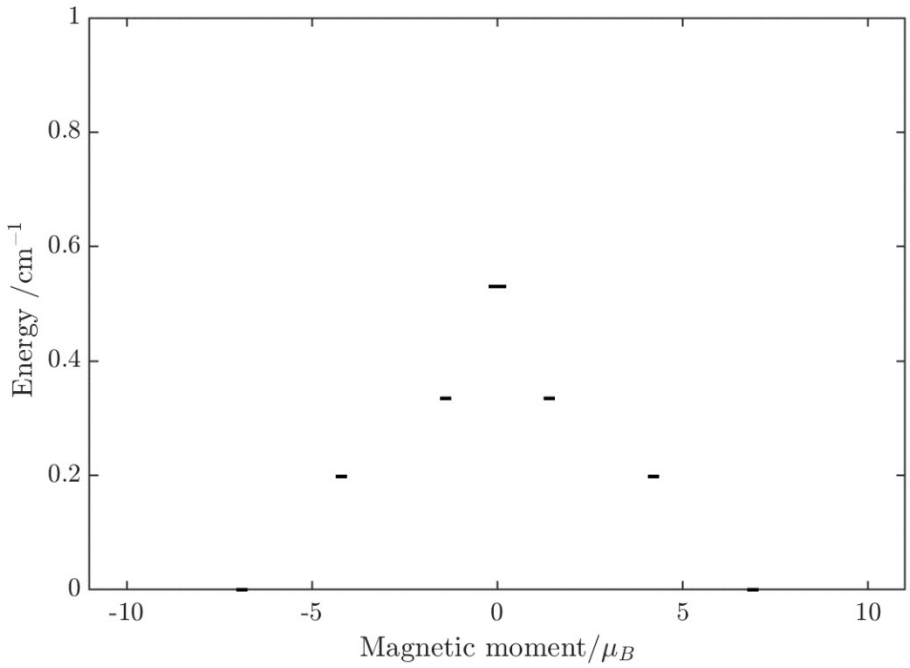

Figure S5. Energies of the low-lying doublets (cm^{-1}) of Gd^{III} center in [FeGd] complex in basis 1.

Table S7. The *g* factors of the low-lying doublets of Gd^{III} center in [FeGd] complex.

Doublets		Basis 1	Basis 2
		g	***g***
1	g_X	0.15985	0.42284
	g_Y	0.22238	0.68593
	g_Z	13.78183	13.51209
2	g_X	2.73740	3.80932
	g_Y	3.73451	5.18294
	g_Z	8.42373	7.09911
3	g_X	2.79567	1.62459
	g_Y	3.78217	2.04471
	g_Z	8.33227	9.27679
4	g_X	0.17405	0.05550
	g_Y	0.24642	0.06982
	g_Z	13.73945	13.87519

Table S8. Energies of the low-lying doublets (cm^{-1}) of Fe^{III} center in [FeGd] complex.

Spin-orbit energies, cm^{-1}	
Basis 1	Basis 2
0.000	0.000
0.000	0.000
0.415	0.394
0.415	0.394
1.227	1.165
1.227	1.165

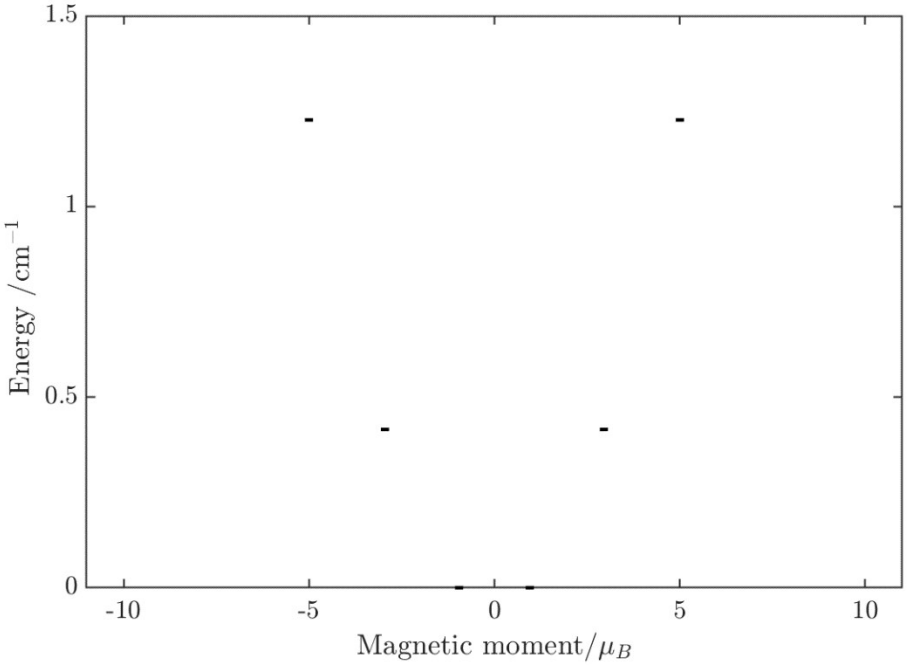

Figure S6. Energies of the low-lying doublets (cm^{-1}) of Fe^{III} center in [FeGd] complex in basis 1.

Table S9. The *g* tensors of the low-lying doublets of Fe^{III} center in [FeGd] complex.

Doublets		Basis 1	Basis 2
		g	***g***
1	g_X	7.21673	7.17258
	g_Y	4.69008	4.74233
	g_Z	1.90723	1.91443
2	g_X	1.21613	1.17151
	g_Y	1.31041	1.25865
	g_Z	5.90455	5.91233
3	g_X	0.01225	0.01087
	g_Y	0.01304	0.01153
	g_Z	10.00299	10.00367

[FeTb] complex:

Table S10. Energies of the lowest doublets (cm^{-1}) of Tb^{III} center in [FeTb] complex.

Spin-orbit energies, cm^{-1}	
Basis 1	Basis 2
0.0000	0.000
0.4490	0.277
40.3807	60.548
42.7626	62.736
81.1407	107.240
100.9895	127.740
114.4760	143.768
148.2008	194.718
150.4164	196.628
268.1518	337.725
268.4580	337.925
384.2096	484.353
384.3101	484.416

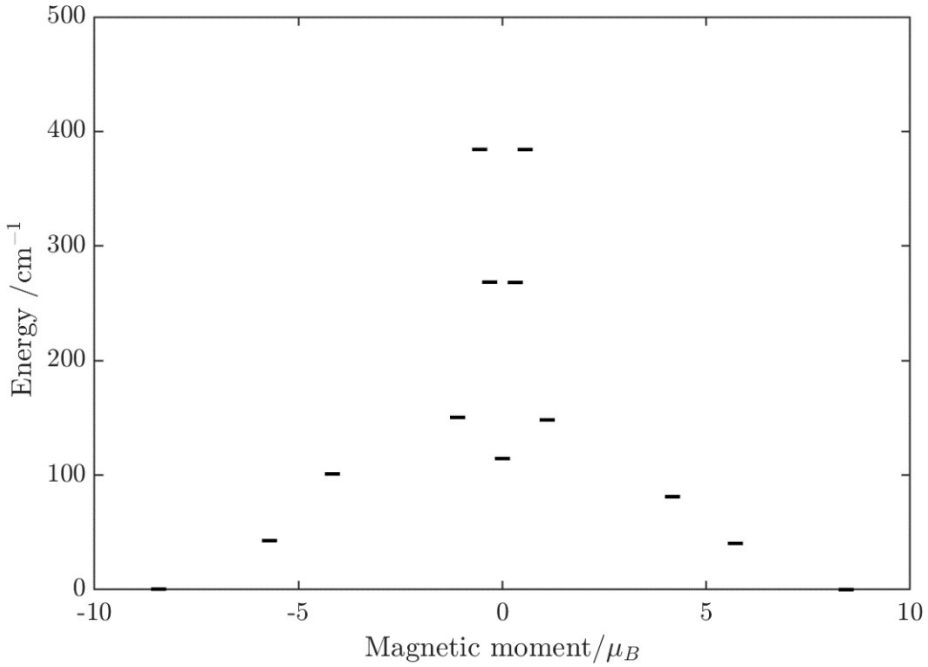

Figure S7. Energies of the lowest doublets (cm^{-1}) of Tb^{III} center in [FeTb] complex in basis 1.

Table S11. The *g* tensors of the lowest doublets of Tb^{III} center in [FeTb] complex.

KD		Basis 1	Basis 2
		g	***g***
1	g_X	0.00000	0.00000
	g_Y	0.00000	0.00000
	g_Z	16.85702	17.15138
2	g_X	0.00000	0.00000
	g_Y	0.00000	0.00000
	g_Z	12.94290	12.95443
3	g_X	0.00000	0.00000
	g_Y	0.00000	0.00000
	g_Z	8.60146	8.25553
4	g_X	0.00000	0.00000
	g_Y	0.00000	0.00000
	g_Z	5.80562	5.92379

Table S12. Energies of the lowest doublets (cm^{-1}) of Fe^{III} center in [FeTb] complex .

Spin-orbit energies, cm^{-1}	
Basis 1	Basis 2
0.000	0.000
0.000	0.000
0.429	0.407
0.429	0.407
1.273	1.208
1.273	1.208

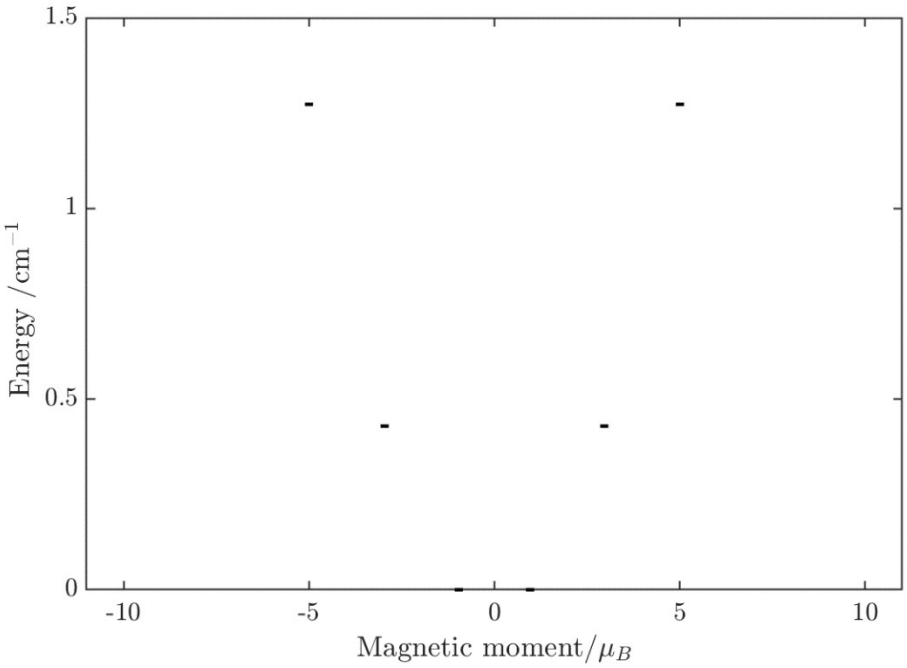

Figure S8. Energies of the lowest doublets (cm^{-1}) of Fe^{III} center in [FeTb] complex in basis 1.

Table S13. The *g* tensors of the lowest doublets (KD) of Fe^{III} center in [FeTb] complex.

Doublets		Basis 1	Basis 2
		g	***g***
1	g_X	7.10952	7.06468
	g_Y	4.81578	4.86801
	g_Z	1.92405	1.93059
2	g_X	1.10640	1.06112
	g_Y	1.18731	1.13554
	g_Z	5.92253	5.92960
3	g_X	0.01260	0.01111
	g_Y	0.01340	0.01178
	g_Z	10.00415	10.00478

[FeDy] complex:

Table S14. Energies of the low-lying Kramers doublets (cm^{-1}) of Dy^{III} center in [FeDy] complex.

Spin-orbit energies, cm^{-1}	
Basis 1	Basis 2
0.000	0.000
70.928	73.369
109.006	109.954
147.885	159.635
163.190	186.650
196.122	226.027
317.135	370.994
443.235	516.558

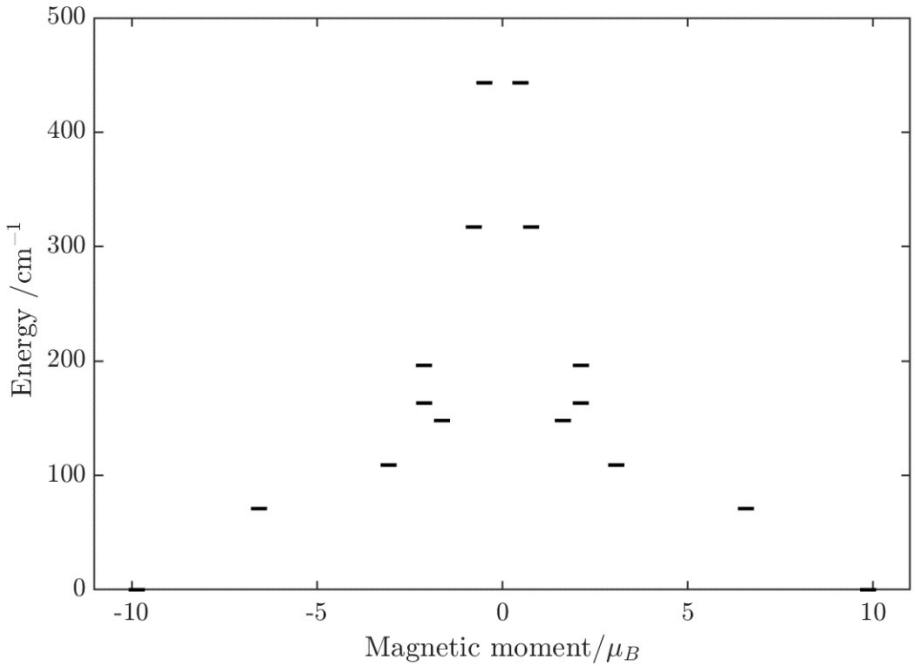

Figure S9. Energies of the low-lying Kramers doublets (cm^{-1}) of Dy^{III} center in [FeDy] complex in basis 1.

Table S15. The *g* factors of the low-lying Kramers doublets of Dy^{III} center in [FeDy] complex.

KD		Basis 1	Basis 2
		g	
1	g_X	0.05165	0.00547
	g_Y	0.06713	0.02665
	g_Z	19.72760	19.73209
2	g_X	0.76793	1.20459
	g_Y	1.36510	3.21875
	g_Z	15.86411	14.62448
3	g_X	3.20886	3.52704
	g_Y	4.82325	4.75569
	g_Z	9.92637	8.23569
4	g_X	1.49678	0.06316
	g_Y	3.22887	3.62145
	g_Z	13.59219	11.89442

Table S16. Energies of the low-lying doublets (cm^{-1}) of Fe^{III} center in [FeDy] complex.

Spin-orbit energies, cm^{-1}	
Basis 1	Basis 2
0.000	0.000
0.000	0.000
0.433	0.409
0.433	0.409
1.283	1.213
1.283	1.213

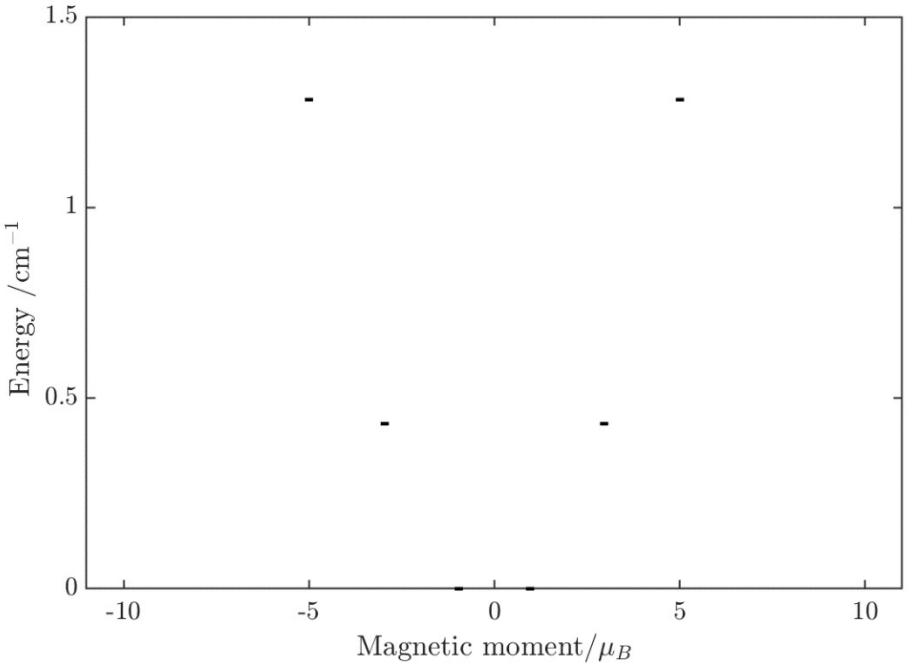

Figure S10. Energies of the low-lying doublets (cm^{-1}) of Fe^{III} center in [FeDy] complex in basis 2.

Table S17. The *g* factors of the low-lying doublets of Fe^{III} center in [FeDy] complex.

Doublets		Basis 1	Basis 2
		g	***g***
1	g_X	7.12816	7.10215
	g_Y	4.79411	4.82464
	g_Z	1.92127	1.92520
2	g_X	1.12260	1.09703
	g_Y	1.21172	1.18069
	g_Z	5.91961	5.92388
3	g_X	0.00226	0.00077
	g_Y	0.00258	0.00100
	g_Z	10.00401	10.00447

2. Electronic and Magnetic Properties of the entire binuclear compounds

The magnetic interactions between Ln^{3+} and the Fe^{3+} ions include contributions from magnetic dipole−dipole and exchange interactions. The exchange coupling was simulated within the Lines model. Magnetic behavior of four interacting Ln^{3+} ions was described using a the Hamiltonian:

$$\hat{H}_{exch} = -J_{Lines}\hat{s}_1\hat{S}_2$$

(Eq. 1)

where $\hat{s}_1$ is the projection operators of the effective spin of Ln ion on the corresponding anisotropy axis, while $\hat{S}_2$ is the spin of the ground state of the Fe^{3+}. J_{Lines} is the parameter of the inter-site magnetic exchange interaction and represent the only fitting parameters of the employed model. The inter-site magnetic dipole-dipole interaction is computed using Eq. (2) and added to the exchange Hamiltonian:

$$\hat{H}_{dip}(i,j) = \mu_{Bohr}^2 \times \frac{\hat{\mu}_i \cdot \hat{\mu}_j - 3(\hat{\mu}_i \cdot n_{ij})(\hat{\mu}_j \cdot n_{ij})}{r_{ij}^3}$$

(Eq. 2)

where $\hat{\mu}_i, \hat{\mu}_j$ are the magnetic moments on the sites i and j, respectively, as obtained from the SINGLE_ANISO single-site calculations, n_{ij} is the normalized vector connecting sites i and j (of length = 1), r_{ij} is the distance between magnetic sites i and j, while μ_{Bohr}^2 is the square Bohr magneton constant, with an approximate value of $\approx$ 0.4329702 cm^{-1}/Tesla. The total Hamiltonian of magnetic interaction is a sum of the two operators:

$$\hat{H}_{total} = \hat{H}_{exch} + \hat{H}_{dip}$$

(Eq. 3)

The low-lying energy spectra obtained by diagonalization of the $\hat{H}_{total}$ and of individual $\hat{H}_{exch}$ and $\hat{H}_{dip}$ are given in the corresponding tables below. The energy splitting gives a rough estimation on the

importance of exchange and dipolar couplings on the total interaction. In all cases it was found that dipole-dipole interactions induces a weaker splitting compared to magnetic exchange.

The eigenstates of $\hat{H}_{total}$ are further used for the description of magnetic susceptibility and molar magnetization of the entire tetranuclear compounds. The parameters J_i were found by minimization of the standard deviation function between measured and calculated magnetic susceptibility. Given that the exchange interaction is rather weak and induces weak splitting, only the low-temperature experimental data points, below 100 K, were considered in the fitting. This task was achieved within the POLY_ANISO code.[2-4]

Further, the magnetic interaction between Fe and Ln in the investigated compounds was estimated by BS-DFT method. These calculations were carried out with ORCA package (version 4.0.0.2 [6]) using B3LYP energy functional and DKH-def2-SVP basis sets. The exchange parameters were estimated by using standard Yamaguchi approach[5]:

$$J = -\frac{E_{HS} - E_{BS}}{\langle \hat{S}^2 \rangle_{HS} - \langle \hat{S}^2 \rangle^{BS}}$$

The energies of low-lying spin-orbit doublets, arising from the magnetic interaction between the ground $S = 5/2$ of the Fe^{III} ion and the ground multiplet ^8S of the Gd^{III} ion in the [FeGd] complex, are shown in Table S19. The corresponding *g*-factors are given in Table S20. The energies of low-lying spin-orbit doublets, arising from the magnetic interaction between the ground $S = 5/2$ of the Fe^{III} ion and the ground crystal-field doublet (effective $S = 1/2$) of the Tb^{III} ion in the [FeTb] complex are shown in Table S22. The corresponding *g*-factors are given in Tables S22. The energies of low-lying spin-orbit doublets, arising from the magnetic interaction between the ground $S = 5/2$ of the Fe^{III} ion and the ground crystal-field doublet (effective $S = 1/2$) of the Dy^{III} ion in the [FeDy] complex are shown in Table S23. The corresponding *g*-factors are given in Tables S24. Note that the experimental χT curve for [FeTb] and [FeDy] were slightly scaled down (Figure S12 and S14) in order to make it consistent with magnetization measurements at low temperatures (Figure S13 and S15).

Table S18. The exchange interaction parameters of complexes.

complex	BS-DFT(cm^{-1})	Poly_aniso(cm^{-1})
[FeGd]	0.71	1.012
[FeTb]	0.85	0.310
[FeDy]	1.23	0.506

We compute standard deviation using a conventional formula:

$$\sigma = \sqrt{\frac{\sum_{i}^{NTemp} \left(XT_{calc}(i) - XT_{measured}(i)\right)^2}{NTemp}}$$

where $NTemp$ is the number of temperature points included in the fitting process. The value of the scaling factor was obtained in the fitting process.
In the table below we give the standard deviation for the fitted parameters, for each compound.

Compound	Parameter			Final value of the standard deviation (σ), using best-fit values		
	J, exchange interaction (cm^{-1})	zJ, mean-field intermolecular interaction (cm^{-1})	Scaling factor, f	$XT_{measured}$ (multiplied with f)	$XT_{measured}$ original	*Powder Magnetisation (3K)* original
FeGd	1.01226	-0.000684	0.981	0.06103	0.27714	0.25964
FeTb	0.31031	-0.027236	0.965	0.14483	0.67455	0.68970
FeDy	0.50613	-0.023293	0.961	0.17677	0.59868	0.23800

[FeGd] complex:

Table S19. Energies of the low-lying states (cm^{-1}) in [FeGd] complex. The total spin *S* corresponds to the isotropic coupling of the $S_{Gd} = 7/2$ of Gd^{III} and $S_{Fe} = 5/2$ of Fe^{III}.

Total spin	**Total Energy, cm^{-1}**	**Exchange Energy only, cm^{-1}**	**Dipolar Energy only, cm^{-1}**
S = 6	0.000000000000	0.00000000	0.00000000
	0.000000566392	0.00033108	0.00171869
	0.482390931628	0.09248655	0.11890664
	0.482436366140	0.10162405	0.12629312
	0.876886139311	0.14795072	0.21626726
	0.877964264320	0.19671350	0.28279182
	1.162595978101	0.20675047	0.31501463
	1.188366369252	0.31781591	0.44431368
	1.322839228069	0.31834082	0.45829775
	1.472060390397	0.49431920	0.50154757
	1.496944638026	0.49432580	0.50589087
	1.839107959852	0.74956742	0.56372776
	1.839882303058	0.74956744	0.59155427
S = 5	6.368047483519	6.24438391	0.66066975
	6.368057832658	6.24456722	0.68224770
	6.768550676925	6.29851253	0.76477584
	6.768811658430	6.30128823	0.84473439
	7.092464689679	6.34214355	0.88580772
	7.094252486407	6.35245969	0.93512556
	7.316635123546	6.37299360	0.95357253
	7.348457120904	6.40219504	1.04369088
	7.460790571018	6.40728268	1.09272534
	7.504122837443	6.44643404	1.10995783
	7.535027560871	6.44699283	1.15758644
S = 4	11.655278226600	11.21070246	1.20327335
	11.655594616670	11.21080093	1.24013408
	11.951992138559	11.32186016	1.24064320
	11.956609125561	11.32569026	1.27972002
	12.153067352538	11.41024262	1.33022522
	12.223153236199	11.44481732	1.34252496
	12.290842101097	11.47463049	1.44406876
	12.508453144766	11.57554791	1.45573588
	12.514393437673	11.57825354	1.50341923
S = 3	15.804476719493	15.08104529	1.50969309
	15.841260939546	15.08135296	1.59435903
	15.961482720346	15.41942266	1.59483185
	16.136344341825	15.43431919	1.85866608
	16.164847600902	15.58471072	1.86259545
	16.515528149563	15.68455198	1.96750324
	16.520289686724	15.71223124	1.97256079
S = 2	18.855752123910	18.09354461	2.04455459
	18.872909586206	18.09657236	2.04692103
	19.131716076181	18.57290566	2.13100192
	19.446708645769	18.64504332	2.13792883
	19.467562560297	18.80494927	2.22850542
S = 1	21.030012669709	20.43197604	2.22959342
	21.251970233926	20.46317408	2.27886548
	21.290840547030	20.52910074	2.28068449

Table S20. The *g* tensors of the low-lying doublets in [FeGd] complex.

Doublets		[FeGd]
		g
1	g_Z	23.93526
2	g_Z	19.82543
3	g_Z	15.55198
4	g_Z	10.73026
6	g_Z	17.67355
7	g_Z	23.57527

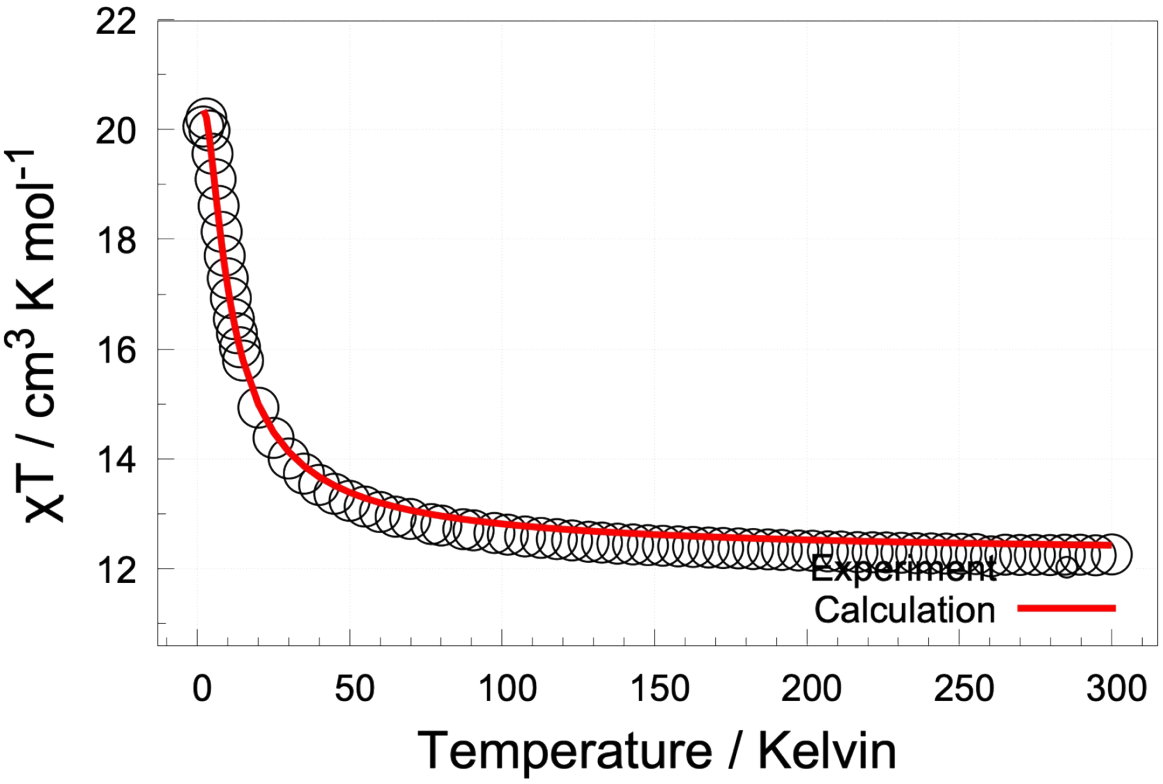

Figure S11. Experimental (circles) vs. calculated (solid red line) magnetic susceptibility of [FeGd].

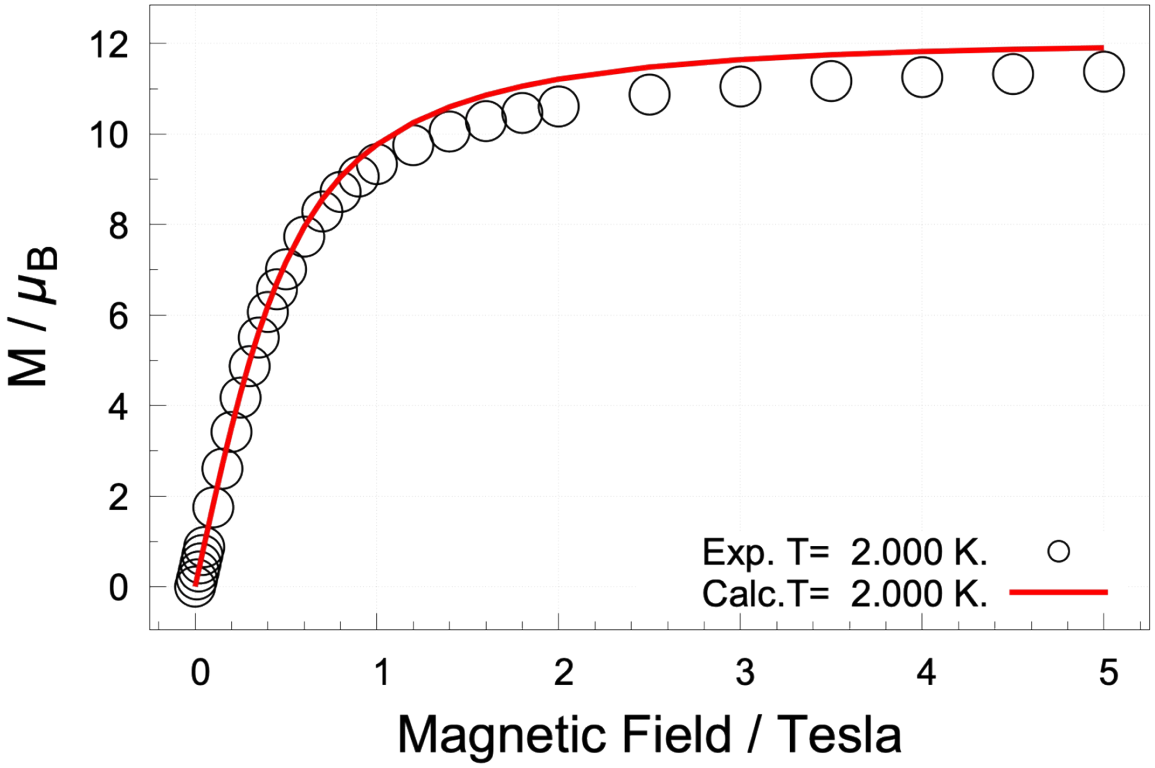
M / μ_B
12
10
8
6
4
2
0
0
1
2
3
4
5
Magnetic Field / Tesla
Exp. T= 2.000 K.
Calc.T= 2.000 K.

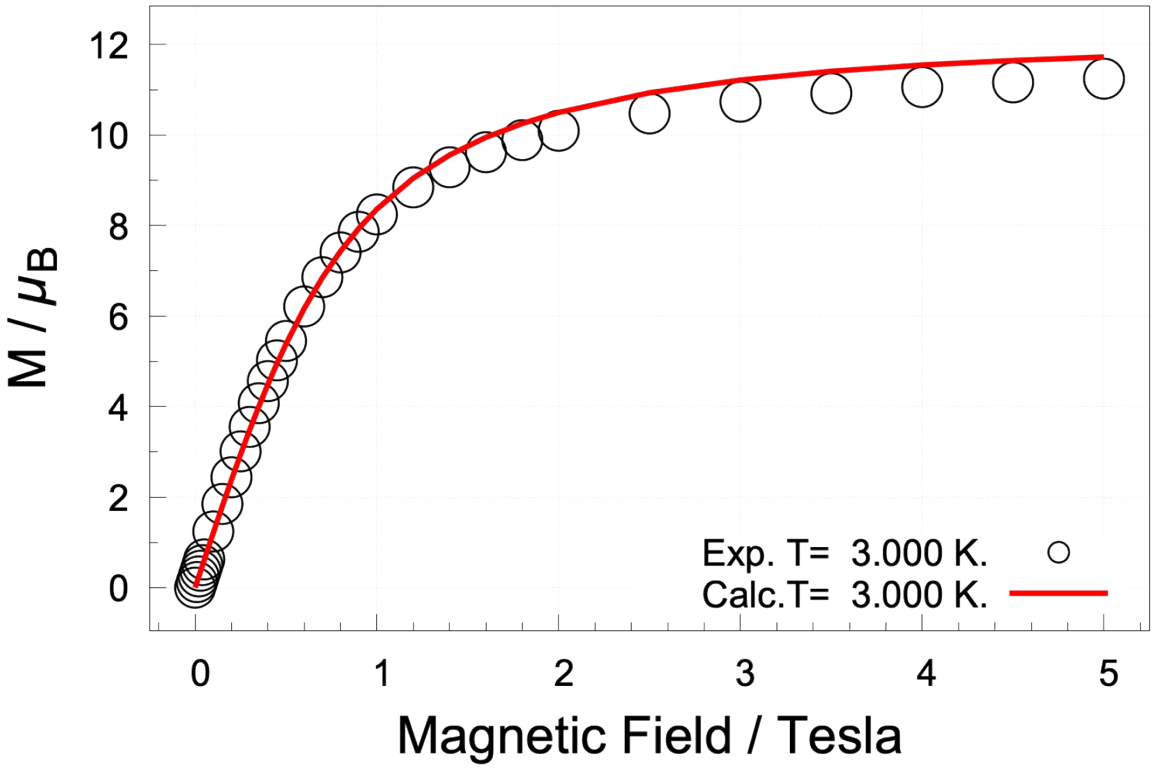
M / μ_B
12
10
8
6
4
2
0
0
1
2
3
4
5
Magnetic Field / Tesla
Exp. T= 3.000 K.
Calc.T= 3.000 K.

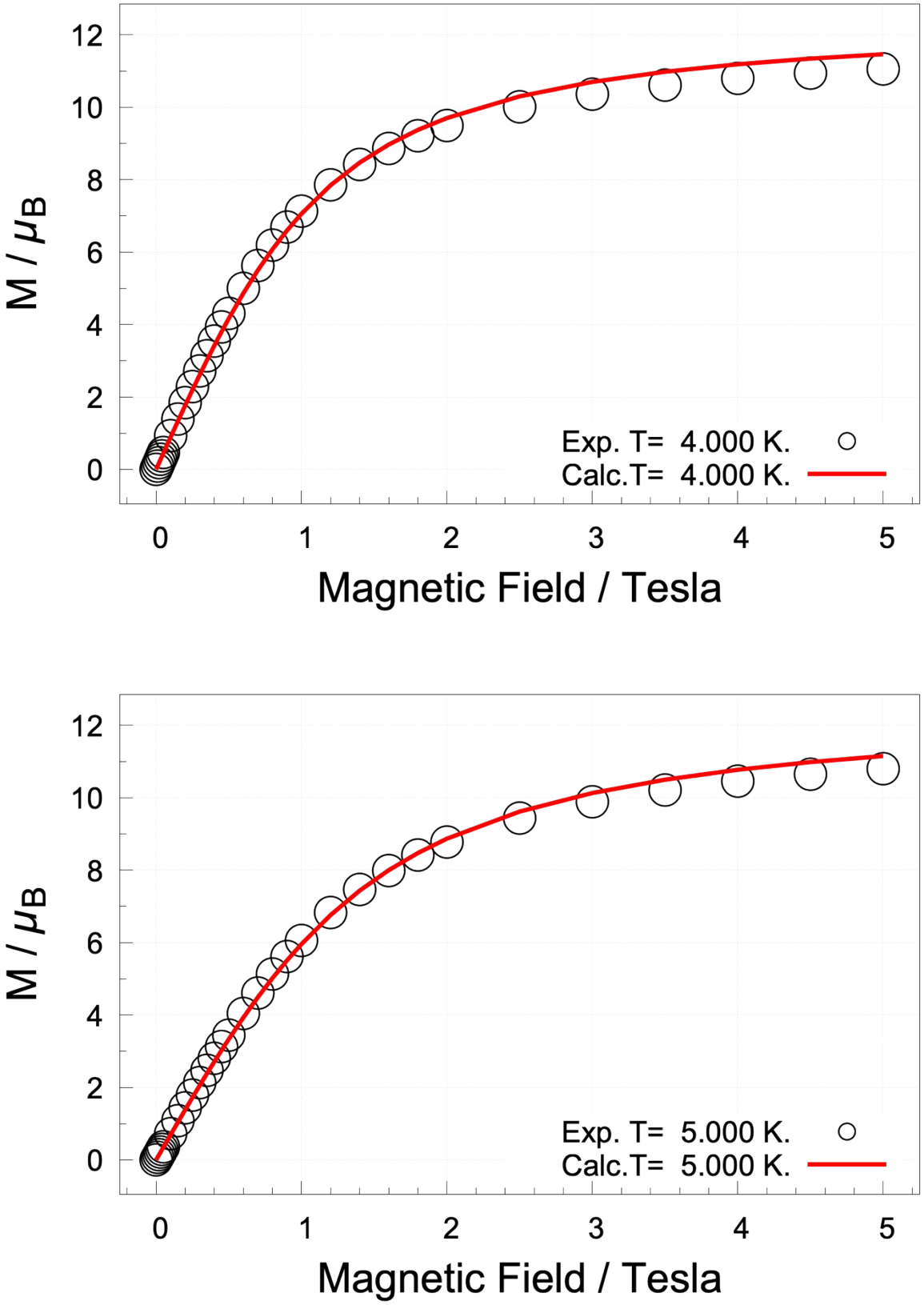

Figure S12. Experimental (circles) vs. calculated (solid red line) field-dependent magnetization of [FeGd] at T = 2K, 3K, 4K and 5K.

[FeTb] complex:

Table S21. Energies of the lowest doublets (cm^{-1}) of [FeTb] center in [FeTb] complex.

Total Energy, cm^{-1}	**Exchange Energy only, cm^{-1}**	**Dipolar Energy only, cm^{-1}**
0.000000000000	0.00000000	0.00000000
0.000000000039	0.00000000	0.00000000
0.925481090303	0.65100351	0.43417590
0.925481090308	0.65100351	0.43417590
1.741871096499	1.19374073	0.95323083
1.741871096508	1.19374073	0.95323083
2.572056287659	2.00123759	1.24840842
2.572056287681	2.00123759	1.24840842
3.540478049706	3.12079068	1.58565145
3.540478049750	3.12079068	1.58565145
4.992876290780	4.71673435	2.19165773
4.992876290824	4.71673435	2.19165773
…	…	…

Table S22. The *g* tensors of the low-lying doublets in [FeTb] complex.

Doublets		[FeTb]
		g
1	g_X	0.100857023
	g_Y	0.127169428
	g_Z	25.24478872
2	g_X	0.960226546
	g_Y	0.968643865
	g_Z	21.911696936
3	g_X	1.463440837
	g_Y	2.605742332
	g_Z	18.783426574
4	g_X	1.373618706
	g_Y	2.976952291
	g_Z	15.035486787
5	g_X	0.426472128
	g_Y	0.440727995
	g_Z	10.895710089
6	g_X	0.006160561
	g_Y	0.007170574
	g_Z	6.811879194

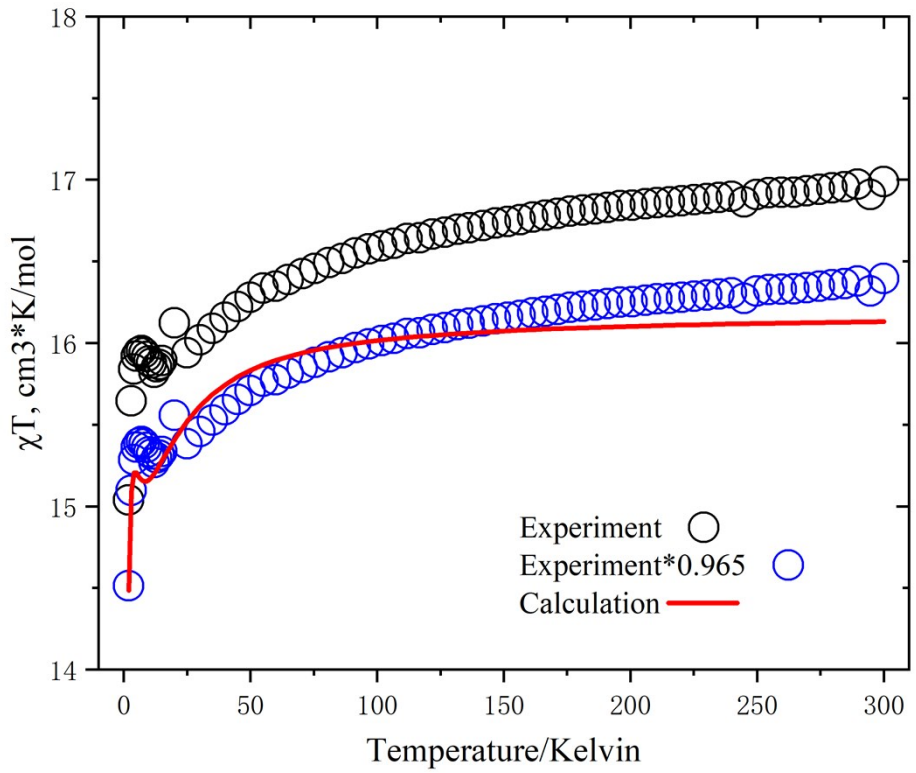

Figure S13. Experimental (circles) vs. calculated (red solid line) magnetic susceptibility of [FeTb].

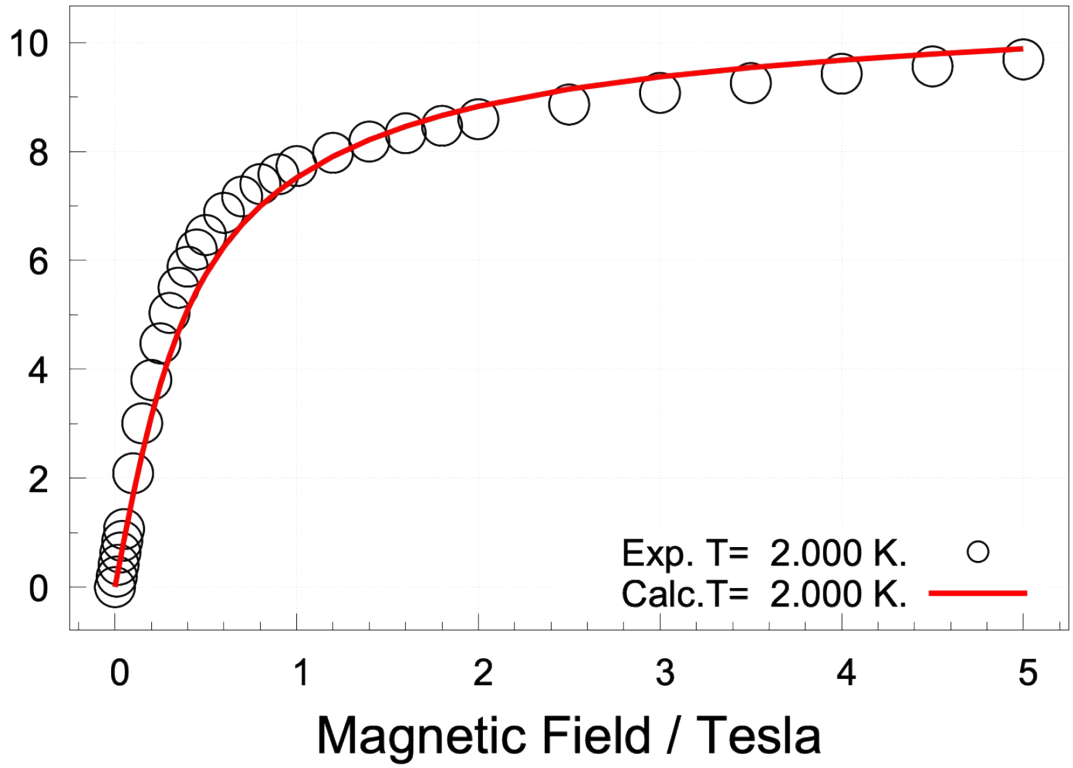

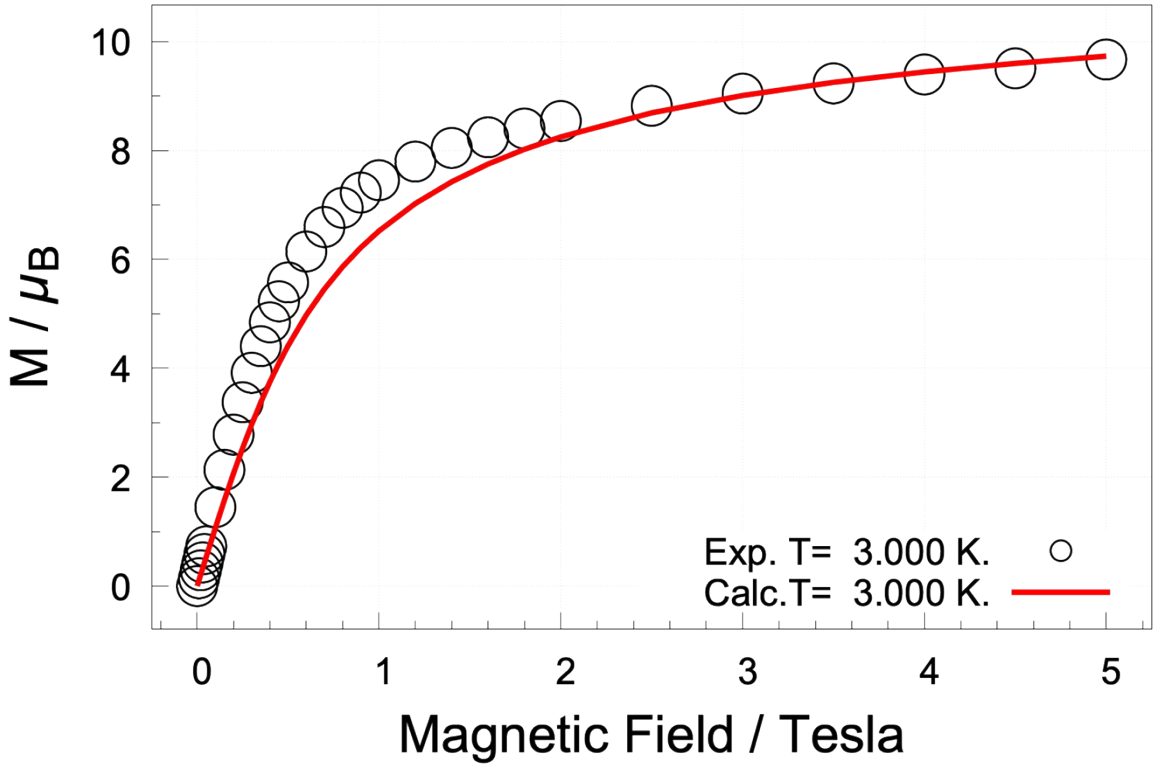
M / μ_B
10
8
6
4
2
0
0
1
2
3
4
5
Magnetic Field / Tesla
Exp. T= 3.000 K.
Calc.T= 3.000 K.

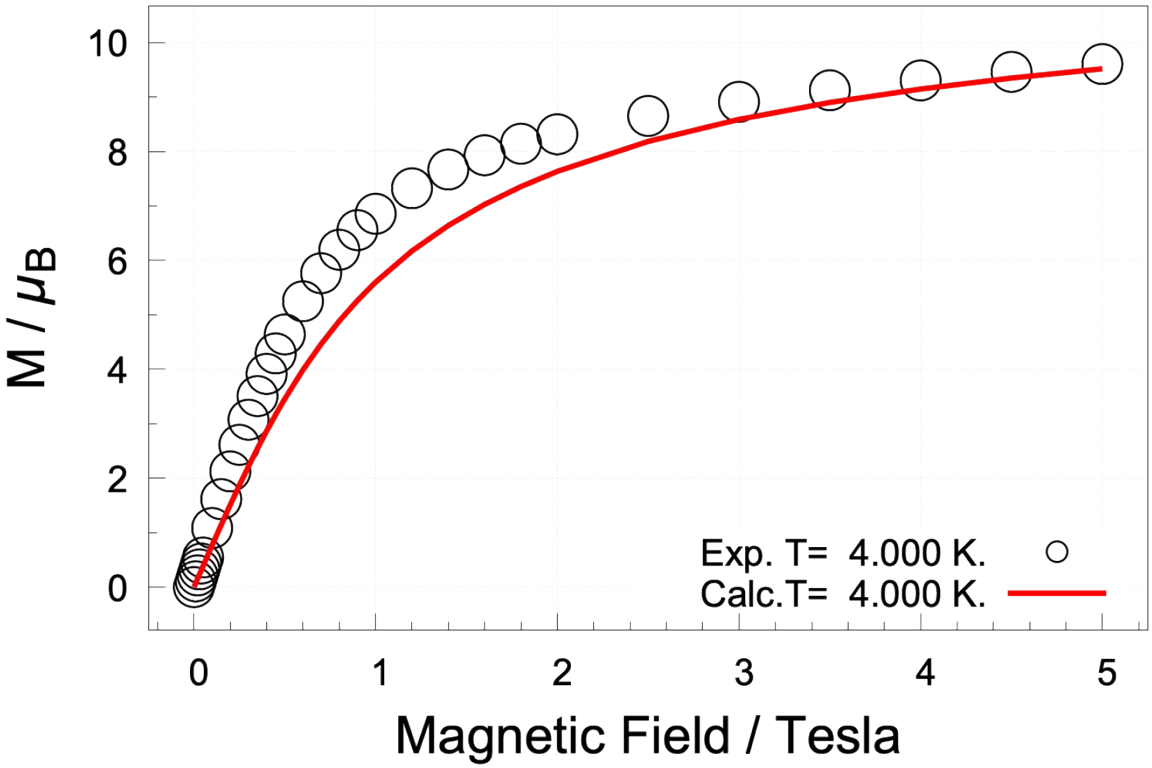
M / μ_B
10
8
6
4
2
0
0
1
2
3
4
5
Magnetic Field / Tesla
Exp. T= 4.000 K.
Calc.T= 4.000 K.

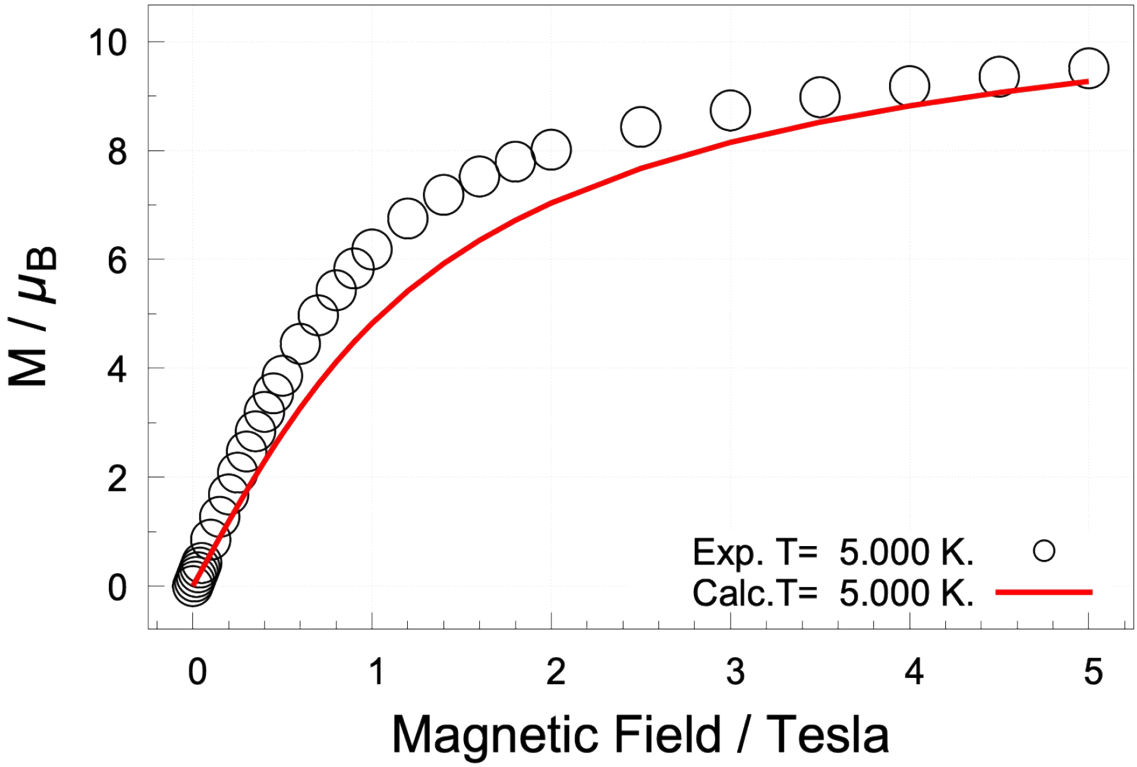

Figure S14. Experimental (circles) vs. calculated (red solid line) field-dependent magnetization of [FeTb] at T = 2K, 3K, 4K and 5K.

[FeDy] complex:

Table S23. Energies and tunneling splitting gaps of the lowest doublets (cm^{-1}) of [FeDy] center in [FeDy] complex.

Total Energy, cm^{-1}	**Tunneling splitting gaps, cm^{-1}**	**Exchange Energy only, cm^{-1}**	**Dipolar Energy only, cm^{-1}**
0.000000000000	0.000046454848	0.00000000	0.00000000
0.000046454848		0.00008919	0.00019318
1.412794235711	0.000758023792	1.19565861	0.41883037
1.413552259503		1.19688412	0.42036289
2.727811614457	0.005622783722	2.32085074	0.78559723
2.733434398179		2.32761476	0.78883602
3.941176255370	0.020107265149	3.43507786	1.26782016
3.961283520519		3.45610964	1.26869680
5.162569239768	0.004749997513	4.76679735	1.33578642
5.167319237281		4.77003157	1.33729046
6.632151289680	0.000202882614	6.47511662	2.30380452
6.632354172294		6.47518607	2.30381618
		…	…

Table S24. The *g* tensors of the low-lying doublets in [FeDy] complex.

Doublets		[FeDy]
		g
1	g_Z	28.96821
2	g_Z	25.45939
3	g_Z	22.17626
4	g_Z	18.71336
5	g_Z	14.17523
6	g_Z	9.79373

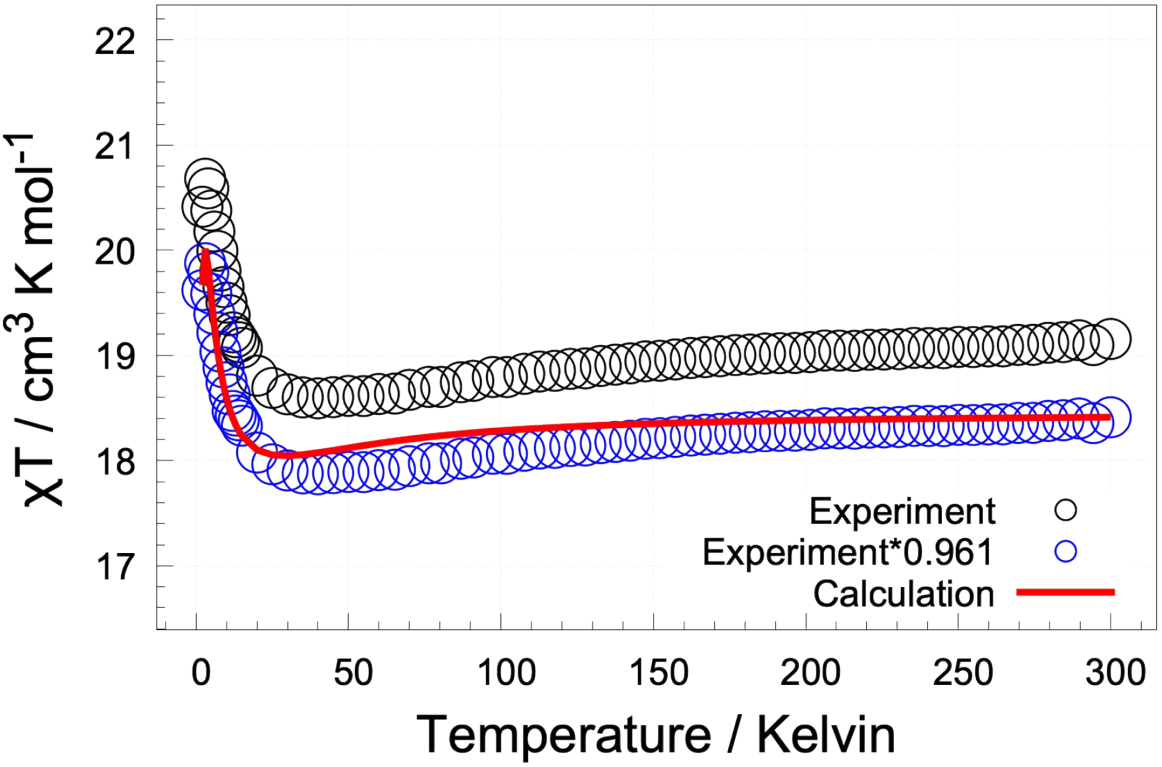

Figure S15. Experimental (circles) vs. calculated (red solid line) magnetic susceptibility of [FeDy].

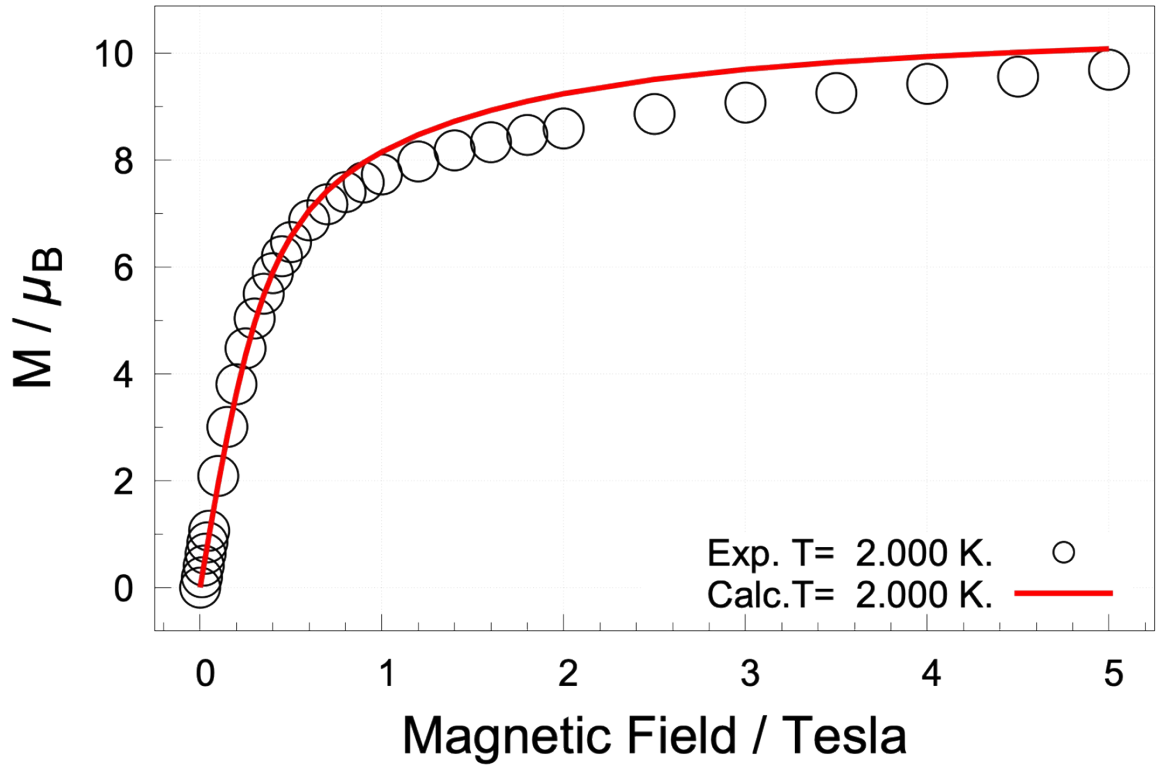

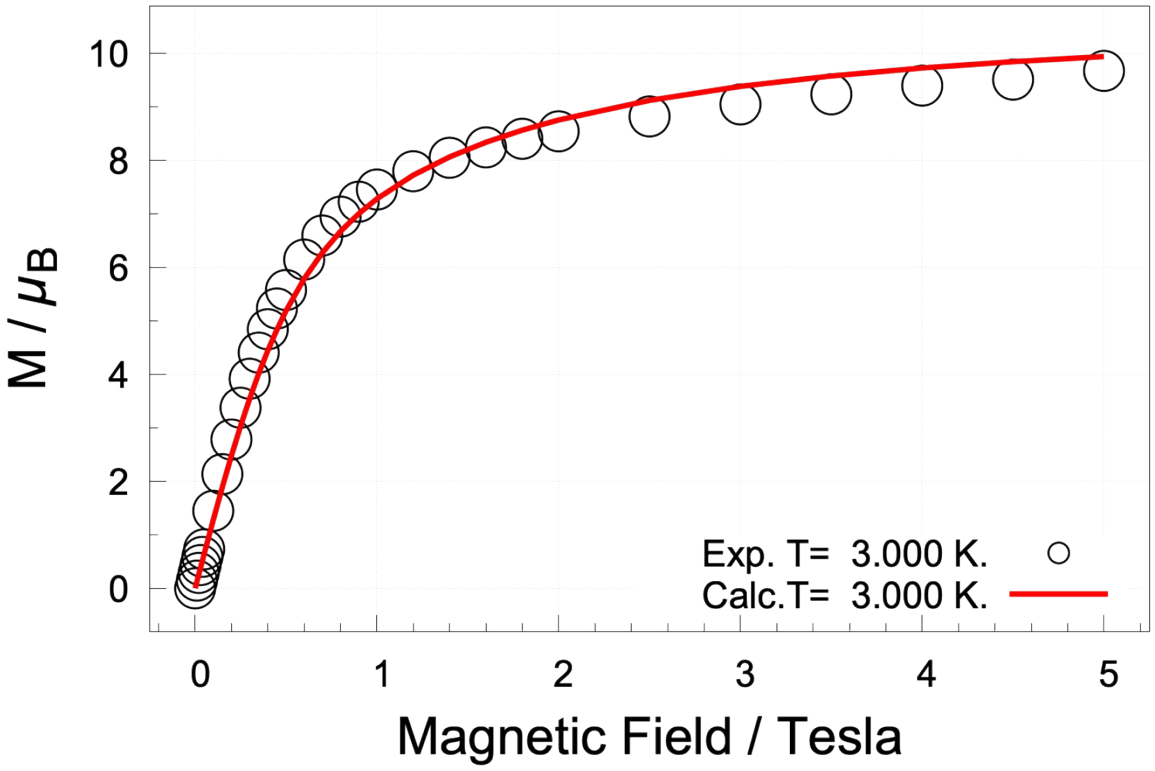
M / μ_B
10
8
6
4
2
0
0
1
2
3
4
5
Magnetic Field / Tesla
Exp. T= 3.000 K.
Calc.T= 3.000 K.

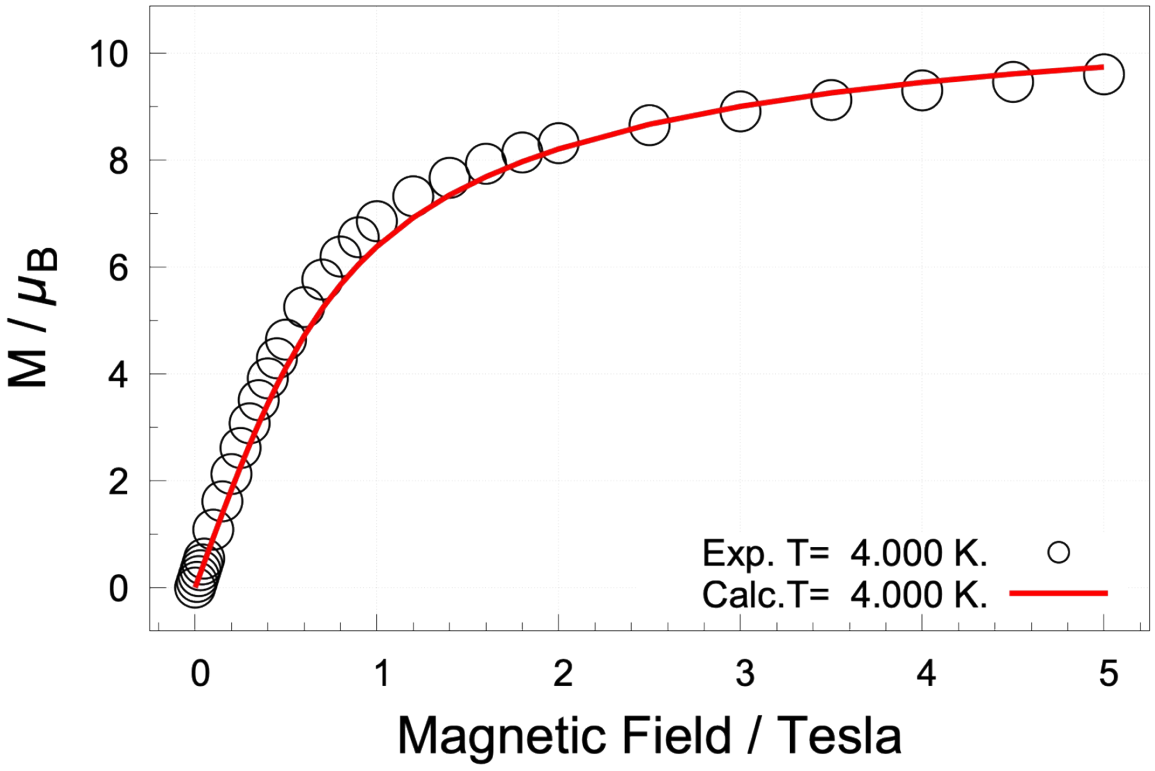
M / μ_B
10
8
6
4
2
0
0
1
2
3
4
5
Magnetic Field / Tesla
Exp. T= 4.000 K.
Calc.T= 4.000 K.

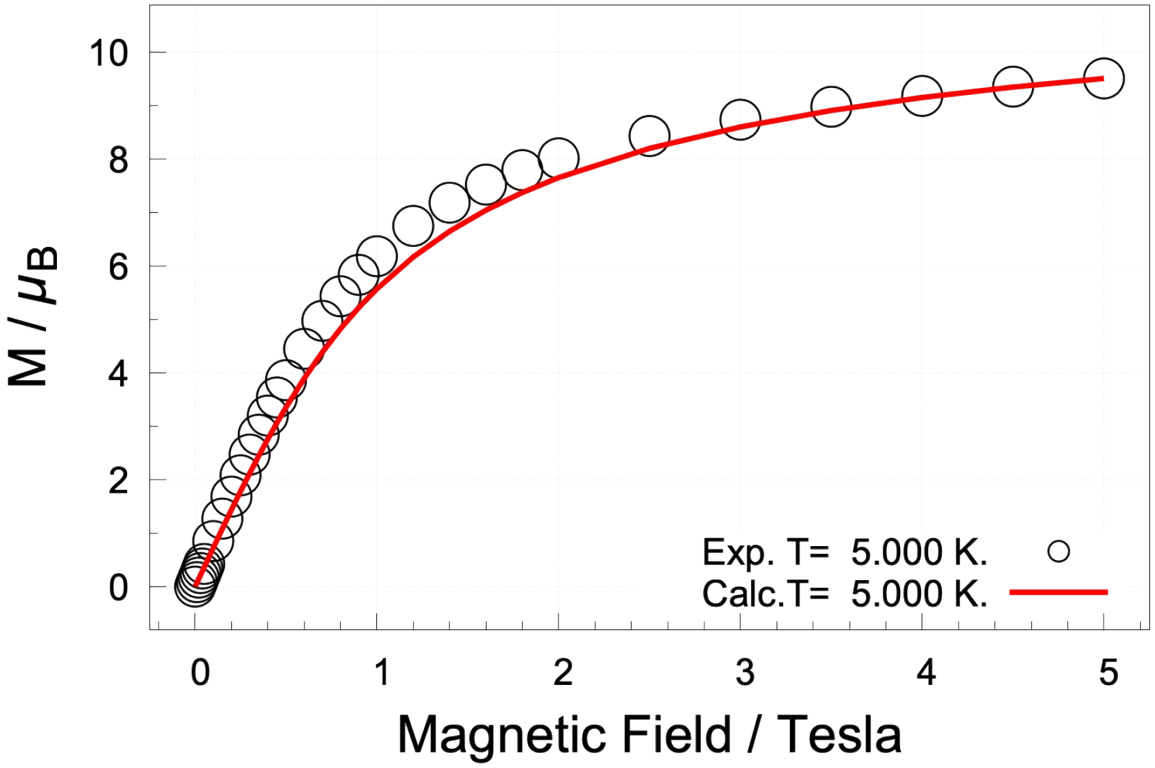

Figure S16. Experimental (circles) vs. calculated (red solid line) field-dependent magnetization of [FeDy] at T = 2K, 3K, 4K and 5K.

References:

[1] F. Aquilante, *et al*. "MOLCAS 8: New capabilities for multiconfigurational quantum chemical calculations across the periodic table." *J. Comp. Chem.* 2016, **37**, 506.

[2] L. Ungur, L. F. Chibotaru, http://www.molcas.org/documentation/manual/.

[3] (a) L. F. Chibotaru, L. Ungur, A. Soncini, *Angew. Chem. Int. Ed.* 2008, **47**, 4126. (b) L. F. Chibotaru, L. Ungur, C. Aronica, H. Elmoll, G. Pilet, D. Luneau, *J. Am. Chem. Soc.* 2008, **130**, 12445.

[4] L. F. Chibotaru, "Theoretical understanding of magnetic anisotropy in molecular nanomagnets", *Struct. Bond* 2015, **164**, 185-230.

[5] M. Shoji , K. Koizumi, Y. Kitagawa, T. Kawakami, S. Yamanaka, M. Okumura, K. Yamaguchi Chemical Physics Letters 432 (2006) 343–347

[6] F.Neese, "Software update: The ORCA program system, version 4.0". Wiley Interdisciplinary Reviews: Computational Molecular Science, 2018 **8** (1): e1327.